

Efficient discrimination between real and complex quantum theories

Josep Batle,^{1,2} Tomasz Bialecki,³ Tomasz Rybotycki,^{4,5} Jakub Tworzydło,³ and Adam Bednorz^{3,*}

¹*Departament de Física UIB i Institut d'Aplicacions Computacionals de Codi Comunitari (IAC3), Campus UIB, E-07122 Palma de Mallorca, Balearic Islands, Spain*

²*CRISP - Centre de Recerca Independent de sa Pobla, 07420 sa Pobla, Balearic Islands, Spain*

³*Faculty of Physics, University of Warsaw, ul. Pasteura 5, PL02-093 Warsaw, Poland*

⁴*Systems Research Institute, Polish Academy of Sciences, 6 Newelska Street, PL01-447 Warsaw, Poland*

⁵*Center for Theoretical Physics, Polish Academy of Sciences, Al. Lotników 32/46, PL02-668 Warsaw, Poland*

We improve the test to show the impossibility of a quantum theory based on real numbers by a larger ratio of complex-to-real bound on a Bell-type parameter. In contrast to previous theoretical and experimental proposals the test requires three setting for the parties A and C , but also six settings for the middle party B , assuming separability of the sources. The bound for this symmetric configuration imposed on a real theory is 14.88 whilst the complex maximum is 18. This large theoretical difference enables us to demonstrate the concomitant experimental violation on IBM quantum computer via a designed quantum network, obtaining as a result 15.44 at more than 80 standard deviations above the real bound.

I. INTRODUCTION

Quantum mechanics is based on complex numbers from its early days [1–3]. Contrasting real- and complex-based quantum theories may bear little relevance for practical purposes, for it is known in several branches of physics that a description based on real numbers alone does not suffice to match experimental results. Thus, real and imaginary parts of the wave function are necessary at least experimentally [4]. It has been pointed out [5–10] that one can replace complex by real numbers by doubling the concomitant complex n -dimensional Hilbert spaces to real-valued ones. However, with this mathematical equivalence comes at a cost of dealing with extra degeneracy of states, where not all are doubled, in particular the ground state. This would not be entail a problem for local phenomena, but separable states consisting of several parties are doubled in each party. Therefore, to reduce the degeneracy one needs extra entanglement in real space, that is, more resources.

Recently, Renou *et al* [11] developed a test designed whether the states separable in complex space can be replaced by an entangled state in real space. It is an approach that essentially conjugates several tools borrowed from quantum information theory. Historically, the path initiated by Bell was to lay the theoretical basis so as to experimentally test the validity of quantum theory as opposed to local variable models (LVM). Along the way, the concepts of non-locality and entanglement gained recognition beyond Bell's purpose and nurtured –together with the tenets of quantum mechanics, unparalleled practical applications in the modern field of quantum computation and information [12]. However, to date no experiment has been able to simultaneously eliminate all possible loopholes. This has important consequences not just in

the arena of fundamental physics (validation of quantum theories), but in the burgeoning field of quantum information science [13–15]. Nevertheless, these drawbacks have not stopped the astonishing progress of the latter.

In Ref. [11] the real separability imposes additional constraints on correlations, leading to an inequality, with lower bound for real states than for complex ones. The test is analogous to the Bell-type tests of nonlocality, involving separated parties. In the real-complex test, there are two sources, P and Q and three observers, A , B , and C , where A and B are connected to the source P while C and B to the source Q . Then B makes a single measurement with 4 outcomes, while A and C make dichotomic measurements for three and six settings, respectively. The violation of the inequality rules out real separability, which has been verified experimentally, [16, 17]. However, the first experiment used photons, which can get lost, so the results were postselected to coincidences. In the second experiment, due to errors, the resulting correlations have been enhanced by the inverse fidelity matrix. The same applies to a recent IBM Quantum test [18].

In the same vein as non-locality tests (that is, the violation of a Bell inequality) can be challenged by LVM with the introduction of loopholes of different nature (locality, detector-efficiency, setting-independence, etc), the experimental tests of real quantum theory are not exempt from them. The locality loophole has been closed recently [19], but the efficiency loophole persisted in all previous experiments. Reduction to four or three settings [20] makes the loophole even harder to close although independence of sources lowers a bit the real bound [21]. In the present contribution, and relying in no apparatus efficiency enhancement whatsoever or fair sampling, we show that the gap between real and complex theories can be actually widened if one allows also six settings for the middle party B with 4 outcomes, which is allowed as the parties are spatially separated. The correlations are generated by permutations of the set 123 corresponding to

* Adam.Bednorz@fuw.edu.pl

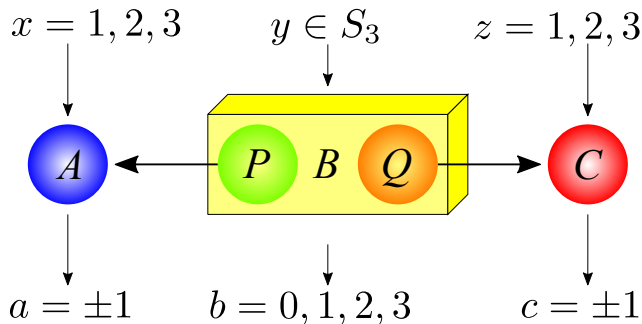


FIG. 1. The setup of the test. The separate sources P and Q generate entangled states. Central parts of these states are measured by B with four possible outcomes b for settings y , corresponding to six permutations of 123 (group S_3), while the left and right parts are measured by observers A and C , with dichotomic outcomes a and c for settings x and z , respectively.

three settings. The real bound can be obtained analytically and it is also confirmed by semidefinite programming (SDP). On the contrary, the quantum bound is 18, obtained by settings of A and C along the main axes of the Bloch sphere, while the B settings are obtained from the maximally entangled state and six rotations of the cube inscribed inside the Bloch sphere.

As opposed to [16, 17], we considerably change the experimental settings (as well as giving rise to new Bell inequalities), upon which we certify our theoretical proposal. Furthermore, we perform our experimental validation in a public venue such as IBM Quantum, making our results highly reproducible without the access to complex experimental facilities. Notice that some universal gates have to be translated into built-in IBM quantum gates.

The present contribution is divided as follows. We begin with the description of the setup and notation. Then we construct the inequality involving six settings of B . Finally we present the demonstration of the violation in a quantum network designed on an IBM Quantum.

II. GENERAL SETUP OF THE TEST

The analyzed system, as in the previous work [11], consists of three observers A , B , and C , depicted in Fig. 1. The sources P and Q are separable, which is an important assumption. In the quantum mechanics based on real numbers, the separability between P and Q leads to tighter bounds on correlations than in full complex space. The Hilbert space can be described as a product of 4 subspaces A , P , Q , C , so that the source states ρ_{AP} and ρ_{QC} are entangled in the respective space, but they remain separated from each other, i.e. the initial state is $\rho = \rho_{AP} \otimes \rho_{QC}$. We can even weaken it to the condition of separability i.e.

$$\rho = \sum_{\lambda} p^{\lambda} \rho_{AP}^{\lambda} \otimes \rho_{QC}^{\lambda} \quad (1)$$

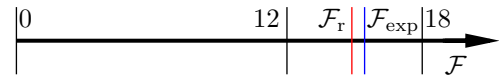


FIG. 2. The value of The Bell-type parameter \mathcal{F} for the IBM demonstration, \mathcal{F}_{exp} (blue), compared to the real quantum bound $\mathcal{F}_r \simeq 14.879$ (red), classical bound 12 and full complex quantum bound 18 (black). The error is below the width of the line.

with some real probability $p^{\lambda} \geq 0$, $\sum_{\lambda} p^{\lambda} = 1$. The separability is the critical assumption as otherwise an additional entanglement between P and Q would make real and complex descriptions indistinguishable. The party B makes the measurement in the PQ space.

We are interested in the correlations

$$\langle A_x B_{yb} C_z \rangle = \text{Tr} \rho A_x \otimes B_{yb} \otimes C_z \quad (2)$$

where A_x and C_z are observables in their respective space while B_y is the entangled observable in the PQ space. The settings are specified by x, y, z while b is the outcome of B . In our case the A/C observables have the values ± 1 so $A_x^2 = C_z^2 = 1$ while $B_{yb} \geq 0$ and $\sum_b B_{yb} = 1$.

The test discriminating real and complex quantum theories will be a linear combination of the above correlations, optimized so that the real bound is much lower than the full complex bound. Except [16], in previous proposals, the observer B had only one setting and four outcomes $b = 0, 1, 2, 3$ [11, 17, 19]. We have made intensive numerical explorations of a wide range of parameters to check if we can beat previous maxima found [11, 20]. The corresponding survey involved a random uniform exploration over the set of coefficients for the Bell inequality, whilst optimizing each complex -and real-valued quantities. Despite extensive numerical efforts, the gap between the real and complex theory turned out to be even smaller than in the original proposal. As we failed to improve previous results, we turned ourselves to the possibility of many settings for the party B .

III. THE TEST WITH SIX SETTINGS OF THE MIDDLE PARTY

The observers A and C can choose one of three settings $x = 1, 2, 3$ and $z = 1, 2, 3$, respectively. We allow the observer B to choose one of six settings enumerated by permutations of the set 123, $y \in S_3 : 123 \rightarrow 123$ denoted by $y \equiv y(1)y(2)y(3)$ i.e. 123, 231, 312, 321, 213, 132, with outcomes $b = 0, 1, 2, 3$. In Appendix A, we prove that the separability in real space implies that

$$\mathcal{F} = \sum_{ybz} \text{sgn } y (-1)^{\delta_{zb} + \delta_{0b}} \langle A_{\sigma(z)} B_{yb} C_z \rangle \leq F_r \quad (3)$$

where

$$\mathcal{F}_r = 2 \left(\sqrt[3]{98 + 18\sqrt{17}} + \sqrt[3]{98 - 18\sqrt{17}} - 1 \right) \simeq 14.8789 \quad (4)$$

It is greater than the classical maximum, 12, based on a LVM, given $A_x, C_z = \pm 1$ and $B_{yb} = 0, 1$. We will show that the full complex maximum is 18. By linearity, it suffices to consider pure initial states $\rho_{AP} = |\psi_{AP}\rangle\langle\psi_{AP}|$, $\rho_{QC} = |\psi_{QC}\rangle\langle\psi_{QC}|$, and measurement $B_b = |\psi_b\rangle\langle\psi_b|$. It is convenient to rewrite (2) in the form of 2×2 trace, using the matrix representation $|\psi\rangle = \sum_{ij} \Psi_{ij} |ij\rangle$, in AP , QC , and PQ space,

$$\langle AB_b C \rangle = \text{Tr} \Psi_b^\dagger \Psi_{AP}^T A^T \Psi_{AP}^* \Psi_b \Psi_{QC}^* C \Psi_{QC}^T \quad (5)$$

Now let us take $A_j = C_j = \sigma_j$ with Pauli matrices σ_j , and the initial states $\Psi_{AP} = \Psi_{QC} = \sigma_2/\sqrt{2}$ and the four outcome states $\Psi_{yb} = R_y \sigma_b \sigma_2/\sqrt{2}$, with rotation R_y on the Bloch sphere. The correlation reads

$$\langle AB_b C \rangle = -\text{Tr} R_y^\dagger A R_y \sigma_b C \sigma_b / 8 \quad (6)$$

since $\sigma_2 A^T \sigma_2 = -A$. We take $R_{123,231,312} = [(\sigma_0 + i\sigma_1 + i\sigma_2 + i\sigma_3)/2]^{0,1,2}$ i.e. the $2\pi/3$ rotation about the principal diagonal (essentially circulating the directions 123) and $R_{132,321,213} = (\sigma_{3,1,2} - \sigma_{2,3,1})/\sqrt{2}$ i.e. π rotations about the in-plane diagonals giving all permutations

$$R^\dagger(A_1, A_2, A_3)R = \text{sgn } y (A_{y(1)}, A_{y(2)}, A_{y(3)}) \quad (7)$$

and $\sigma_b \sigma_j \sigma_b = (-1)^{\delta_{jb} + \delta_{0b} + 1} \sigma_j$. All in all each correlation gives $1/4$ for each x, z, y, b and 1 summed over b , which is 18 in total.

IV. IMPLEMENTATION ON IBM

We have demonstrated the above test on IBM Quantum, exceeding the real bound as shown in Fig. 2. The implementation uses 4 qubits, corresponding to $APQC$, connected by $CNOT$ gates (or equivalent) The initial state of each of four is $|0\rangle$. The initial state AP and QC is realized by $CNOT$ gates, i.e. $CNOT_\downarrow(Y_- I)|00\rangle$, using the convention for tensors that $(AB)|ab\rangle$ means $(A|a\rangle)(B|b\rangle)$ and $V_\pm = \exp(\mp i\pi V/4)$ with Pauli gates $X, Y, Z = \sigma_{1,2,3}$. the $CNOT$ gate reads

$$CNOT_\downarrow = \begin{pmatrix} I & 0 \\ 0 & X \end{pmatrix} = \begin{pmatrix} 1 & 0 & 0 & 0 \\ 0 & 1 & 0 & 0 \\ 0 & 0 & 0 & 1 \\ 0 & 0 & 1 & 0 \end{pmatrix} \quad (8)$$

in the basis $|00\rangle, |01\rangle, |10\rangle, |11\rangle$. The measurement operators $A_j = G_j^\dagger Z G_j = C_j$ with $G_1 = I, G_2 = X_+, G_3 = X_+ Z_+$. Operationally Z is measured as a difference of $|0\rangle$ and $|1\rangle$ population. The outcome in PQ space is defined $B_{yb} = G_y^\dagger M_{yb} G_y'$ with

$$G_y' = (Y_- I) CNOT_\downarrow (G_y I) \quad (9)$$

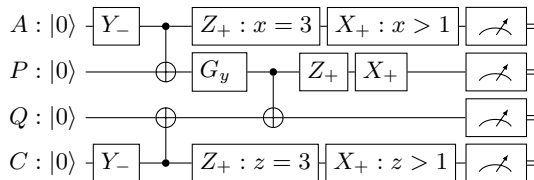


FIG. 3. The circuit implementing the complex-real test for the correlation $\langle A_x B_{yb} C_z \rangle$. The gate G_y corresponds to the appropriate permutation. The $CNOT_\downarrow|ab\rangle$ gate links $a = \bullet$ with $b = \oplus$.

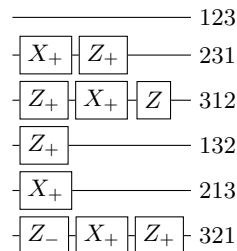


FIG. 4. The gate G_y for each permutation

and $G_{123} = I, G_{231} = Z_+ X_+, G_{312} = Z X_+ Z_+, G_{132} = Z_+, G_{213} = X_+, G_{321} = Y_+$. The projection $M = |m\rangle\langle m|$ given by the PQ two-qubit state is specified in Table I.

We performed the test on *ibm_brisbane*, qubits 47 (A), 48 (P), 49 (Q), 55 (C), with native single qubit gates X_+ phase shifts Z_\pm and $CNOT$ gates transpiled by the native ECR gates, see Fig. 6 and Appendix B. The errors of ECR gates $48 \rightarrow 47, 48 \rightarrow 49, 55 \rightarrow 49$, are $5.2 \cdot 10^{-3}, 1.1 \cdot 10^{-2}, 1.3 \cdot 10^{-2}$, respectively. To determine the total error, we assume independence between experiments. For a given x, y and z the contribution to the error is

$$N \langle \Delta \mathcal{F}_{xyz}^2 \rangle = 1 - F_{xyz}^2 \quad (10)$$

where

$$\mathcal{F}_{xyz} = \sum_b (-1)^{\delta_{zb} + \delta_{0b}} \langle A_x B_{yb} C_z \rangle, \quad (11)$$

at $x = y(z)$, is the partial witness contribution, omitting global signs. Here N is the total number of trials. Then

$$\langle \Delta \mathcal{F}^2 \rangle = \sum_{xyz} \langle \Delta \mathcal{F}_{xyz}^2 \rangle \quad (12)$$

y	$ 00\rangle$	$ 01\rangle$	$ 10\rangle$	$ 11\rangle$
123	2	1	3	0
231	3	0	2	1
312	0	3	1	2
132	0	3	1	2
213	0	3	1	2
321	1	2	0	3

TABLE I. The outcome b depending on the permutations y and the states pq of the qubits P and Q .

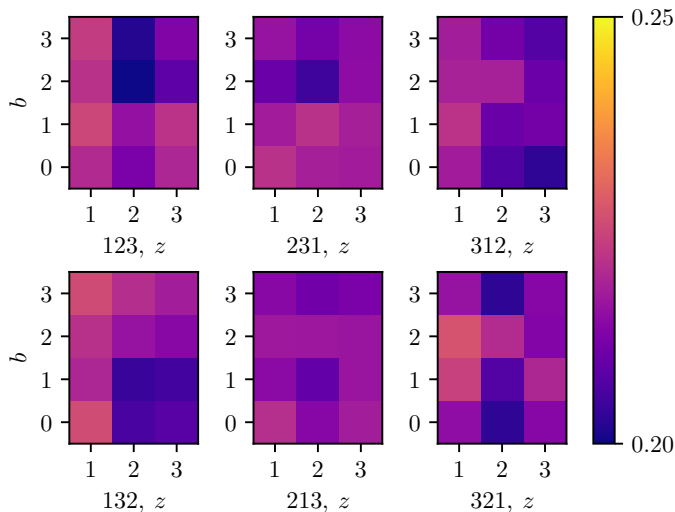


FIG. 5. The correlations $\text{sgn } y (-1)^{\delta_{jb} + \delta_{ob}} \langle A_{y(z)} B_{yb} C_z \rangle$ for all values z, b, y , from the IBM Quantum demonstration. In the ideal case, they are all equal 0.25.

device/qubit	freq. (GHz)	r/a error
47(A)	4.770	$5.5 \cdot 10^{-3}$
48(P)	4.844	$1.3 \cdot 10^{-2}$
49(Q)	4.697	$9.1 \cdot 10^{-3}$
55(C)	4.837	$9.5 \cdot 10^{-3}$

TABLE II. The characteristics of the qubits used in the demonstration, frequency between 0 and 1 level, read-out/assignment error. The duration of the single gate pulse is always 35ns.

Using 6 jobs, 20000 shots for all 18 correlations we obtained the value 15.4436 ± 0.0066 which is above the real threshold by more than 80 standard deviations. The individual correlations are presented in Fig. 5 while the obtained value related to the other bounds is shown in Fig. 2. We checked also no signaling, i.e. if a party's setting affects results of other party when ignoring its outcomes and no significant disagreement have been found. The

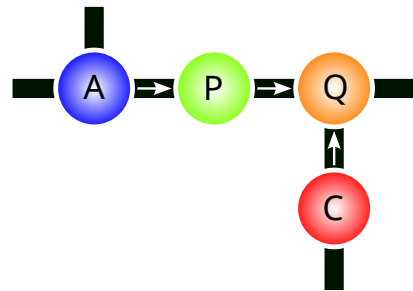


FIG. 6. The actual topology of qubits used in the test on *ibm_brisbane* for the circuit in Fig. 3. The black connections indicate two-qubit gates linking the test qubits and external ones. The arrows show the direction of *ECR* gates between the test qubits (see Appendix B).

data and scripts are publicly available [22].

V. CONCLUSION

We have shown that the discrimination between real complex quantum theories can be tested with non-ideal resources using a public available quantum computer, without additional steps such as inverse fidelity matrix. An open question remains if the test and bound is absolutely optimal (our computational efforts did not elucidate that question). One can also try to perform the test at larger distances to close the locality loophole simultaneously. Be it as it may, we believe that the answer to the question of whether quantum mechanics needs complex numbers or not is now undoubtedly answered in the positive.

ACKNOWLEDGMENTS

We thank M.-O. Renou for inspiring discussions. The results have been created using IBM Quantum. The views expressed are those of the authors and do not reflect the official policy or position of IBM or the IBM Quantum team. TR acknowledges the financial support by TEAM-NET project co-financed by EU within the Smart Growth Operational Programme (contract no. POIR.04.04.00-00-17C1/18-00).

Appendix A: Derivation of the bound for real separable states

We shall derive the bound given by Eqs. (3) and (4). Let us consider the following sum of squares times non-negative operators,

$$\begin{aligned}
0 \leq & \sum_{yb} [(A_{\sigma(1)}C_1(-1)^{\delta_{2b}+\delta_{3b}} + A_{y(2)}C_2(-1)^{\delta_{1b}+\delta_{3b}} + A_{y(3)}C_3(-1)^{\delta_{1b}+\delta_{2b}} + x \operatorname{sgn} y)^2 B_{yb} \\
& + ((\operatorname{sgn} y A_{y(1)}C_1 - A_{y(2)}C_2 A_{y(3)}C_3)/2t - \operatorname{sgn} y t A_{y(2)}C_2(-1)^{\delta_{1b}+\delta_{2b}} + (-1)^{\delta_{2k}+\delta_{3b}}t)^2 B_{yb} \\
& + ((\operatorname{sgn} y A_{y(2)}C_2 - A_{y(3)}C_3 A_{y(1)}C_1)/2t - \operatorname{sgn} y t A_{y(3)}C_3(-1)^{\delta_{2b}+\delta_{3b}} + (-1)^{\delta_{3k}+\delta_{1k}}t)^2 B_{yb} \\
& + ((\operatorname{sgn} y A_{y(3)}C_3 - A_{y(1)}C_1 A_{y(2)}C_2)/2t - \operatorname{sgn} y t A_{y(1)}C_1(-1)^{\delta_{3b}+\delta_{1b}} + (-1)^{\delta_{1b}+\delta_{2b}}t)^2 B_{yb}] \quad (A1)
\end{aligned}$$

Here $0 \leq B_{\sigma b} \leq 1$ but $\sum_b B_{\sigma b} = 1$, while $A^2 = C^2 = 1$ and the square for nonsymmetric matrices should be operationally understood as $O^2 = O^T O$. Then

$$\begin{aligned}
& 3 + x^2 + 6(t^2 + 1/4t^2) - \sum_{yy'} \operatorname{sgn} yy' A_{y(1)}A_{y(2)}A_{y(3)}C_{y'(1)}C_{y'(2)}C_{y'(3)} \\
\geq & (t^2 - x - 1) \sum_{yb} \operatorname{sgn} y [(A_{y(1)}C_1(-1)^{\delta_{2b}+\delta_{3b}} + A_{y(2)}C_2(-1)^{\delta_{1b}+\delta_{3b}} + A_{y(3)}C_3(-1)^{\delta_{1b}+\delta_{2b}}]. \quad (A2)
\end{aligned}$$

Since the real separability implies equality with partial transpose, i.e. the AC density matrix satisfies $\rho_{aa'cc'} = \rho_{a'ac'c}$ then the sum over permutations cancels. To get the best constraint we have to minimize

$$\mathcal{F}_r = 3 \frac{3 + x^2 + 6(t^2 + 1/4t^2)}{x + 1 - t^2} \quad (A3)$$

over $x \geq t^2 - 1$ as

$$\mathcal{F}_r \geq \sum_{ybz} \operatorname{sgn} y (-1)^{\delta_{zb}+\delta_{0b}} \langle A_{y(z)} B_{yb} C_z \rangle \quad (A4)$$

The analysis of the extrema gives the minimum for

$$t^2 = \frac{15 + 9x}{2x^3 + 10x^2 + 6x - 6} \quad (A5)$$

with x being the real root of

$$x^3 + x^2 - 5x - 9 = 0 \quad (A6)$$

and

$$\begin{aligned}
\mathcal{F}_r &= 6 \frac{2x^3 + x^2 + 9}{(x-1)(3x+5)} = 6 \frac{2x^3 + x^2 + 9 + (x^3 + x^2 - 5x - 9)}{(x-1)(3x+5)} \\
&= 6x = 2 \left(\sqrt[3]{98 + 18\sqrt{17}} + \sqrt[3]{98 - 18\sqrt{17}} - 1 \right) \\
&\simeq 14.87889449253087 \quad (A7)
\end{aligned}$$

by Cardano formula. We additionally confirmed the bound by SDP code, see [22, 23], by examining formal sums of squares of expressions containing products up to 2 observables A and C , i.e. $1, A_x, C_z, A_x A_{x'}, C_z C_{z'}, A_x C_z, A_x A_{x'} C_z, A_x C_z C_{z'},$ and $A_x A_{x'} C_z C_{z'}$.

Appendix B: Transpiling $CNOT$ gates by ECR gates

The IBM Quantum devices (*ibm_brisbane*) use transmon qubits [24] a native two-qubit gate Echoed Cross Resonance (ECR) instead of $CNOT$. However, one can transpile the latter by the former, adding single qubits gates. We shall use Pauli matrices in the basis $|0\rangle, |1\rangle$,

$$X = \begin{pmatrix} 0 & 1 \\ 1 & 0 \end{pmatrix}, Y = \begin{pmatrix} 0 & -i \\ i & 0 \end{pmatrix}, Z = \begin{pmatrix} 1 & 0 \\ 0 & -1 \end{pmatrix}, I = \begin{pmatrix} 1 & 0 \\ 0 & 1 \end{pmatrix}. \quad (B1)$$



FIG. 7. The notation of the ECR gate in the convention $ECR_{\downarrow}|ab\rangle$

We also denote two-qubits gates by \downarrow and \uparrow , which mean the direction of the gate (it is not symmetric), i.e. $\langle a'b'|G_{\uparrow}|ab\rangle = \langle b'a'|G_{\downarrow}|ba\rangle$.

The ECR gate acts on the states $|ab\rangle$ as (Fig. 7)

$$\begin{aligned}
ECR_{\downarrow} &= (XI - YX)/\sqrt{2} = CR^{-}(XI)CR^{+} = \\
& \begin{pmatrix} 0 & X_{-} \\ X_{+} & 0 \end{pmatrix} = \begin{pmatrix} 0 & 0 & 1 & i \\ 0 & 0 & i & 1 \\ 1 & -i & 0 & 0 \\ -i & 1 & 0 & 0 \end{pmatrix} / \sqrt{2} \quad (B2)
\end{aligned}$$

in the basis $|00\rangle, |01\rangle, |10\rangle, |11\rangle$ where the native gate is

$$X_{+} = X_{\pi/2} = (I - iX)/\sqrt{2} = \begin{pmatrix} 1 & -i \\ -i & 1 \end{pmatrix} / \sqrt{2} \quad (B3)$$

and $X_{-} = X_{-\pi/2} = ZX_{+}Z$, with opposite Crossed Resonance gates

$$CR^{\pm} = (ZX)_{\pm\pi/4}, \quad (B4)$$

using the convention $V_{\theta} = \exp(-i\theta V/2) = \cos(\theta/2) - iV \sin(\theta/2)$ if $V^2 = I$ or II .

The gate is its inverse, i.e. $ECR_{\downarrow}ECR_{\downarrow} = II$.

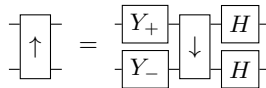
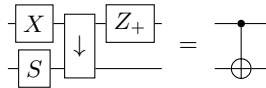
Note that $Z_{\theta} = \exp(-i\theta Z/2) = \operatorname{diag}(e^{-i\theta/2}, e^{i\theta/2})$ is a virtual gate adding essentially the phase shift to next gates. [25] ECR gates can be reversed, i.e., for $a \leftrightarrow b$, (Fig. 8)

$$ECR_{\uparrow} = (IX - XY)/\sqrt{2} = (HH)ECR_{\downarrow}(Y_{+}Y_{-}) \quad (B5)$$

denoting $V_{\pm} = V_{\pm\pi/2}$, and Hadamard gate

$$H = (Z + X)/\sqrt{2} = Z_{+}X_{+}Z_{+} = \begin{pmatrix} 1 & 1 \\ 1 & -1 \end{pmatrix} / \sqrt{2} \quad (B6)$$

and $Z_{\pm}SZ_{\mp} = Y_{\pm}$, with $Y_{+} = HZ$ and $Y_{-} = ZH$.

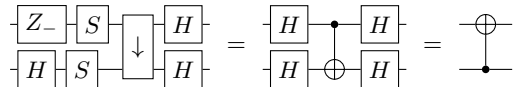
FIG. 8. The ECR_{\uparrow} gate expressed by ECR_{\downarrow} .FIG. 9. The $CNOT_{\downarrow}$ gate expressed by ECR_{\downarrow} .

The CNOT gate can be expressed by ECR (Fig. 9)

$$CNOT_{\downarrow} = (II + ZI + IX - ZX)/2 = \begin{pmatrix} 1 & 0 & 0 & 0 \\ 0 & 1 & 0 & 0 \\ 0 & 0 & 0 & 1 \\ 0 & 0 & 1 & 0 \end{pmatrix} = (Z_+I)ECR_{\downarrow}(XS) \quad (B7)$$

while its reverse reads (Fig. 10)

$$CNOT_{\uparrow} = (II + IZ + XI - XZ)/2 = \begin{pmatrix} 1 & 0 & 0 & 0 \\ 0 & 0 & 0 & 1 \\ 0 & 0 & 1 & 0 \\ 0 & 1 & 0 & 0 \end{pmatrix} = (HH)CNOT_{\downarrow}(HH) = (HH)ECR_{\downarrow}(SS)(Z_-H) \quad (B8)$$

FIG. 10. The $CNOT_{\uparrow}$ gate expressed by ECR_{\downarrow} .

- [1] M. Born and P. Jordan, Zur Quantenmechanik, *Z. Phys.* **34**, 858 (1925).
- [2] M. Born, W. Heisenberg, and P. Jordan, Zur Quantenmechanik II, *Z. Phys.* **35**, 557 (1926).
- [3] E. Schrödinger, An undulatory theory of the mechanics of atoms and molecules, *Phys. Rev* **28**, 1049 (1926).
- [4] J. S. Lundeen, B. Sutherland, A. Patel, C. Stewart, and C. Bamber, Direct measurement of the quantum wavefunction, *Nature* (London) **474**, 188 (2011).
- [5] G. Birkhoff and J. Von Neumann, *Ann. Math.* **37**, 823 (1936).
- [6] E. C. G. Stueckelberg, Quantum theory in real Hilbert space, *Helv. Phys. Acta* **33**, 727 (1960).
- [7] E. C. G. Stueckelberg and M. Guenin, Quantum theory in real Hilbert space II, *Helv. Phys. Acta* **34**, 621 (1961).
- [8] F. J. Dyson, The threefold way. Algebraic structure of symmetry groups and ensembles in quantum mechanics, *J. Math. Phys. (N.Y.)* **3**, 1199 (1962).
- [9] K. F. Pal and T. Vertesi, Efficiency of higher-dimensional Hilbert spaces for the violation of Bell inequalities, *Phys. Rev. A* **77**, 042105 (2008).
- [10] M. McKague, M. Mosca, and N. Gisin, Simulating Quantum Systems Using Real Hilbert Spaces, *Phys. Rev. Lett.* **102**, 020505 (2009).
- [11] M.-O. Renou, D. Trillo, M. Weilenmann, Le Phuc Think, A. Tavakoli, Nicolas Gisin, A. Acin and M. Navascues, Quantum theory based on real numbers can be experimentally falsified, *Nature* **600**, 625 (2021)
- [12] D. Bouwmeester, A. K. Ekert, A. Zeilinger (Eds.), *The Physics of Quantum Information* (Springer, Berlin, 2000); M. L. Nielsen and I. L. Chuang, *Quantum Computation and Quantum Information* (Cambridge University Press, Cambridge, UK, 2010); J. D. Hidary, *Quantum Computing: An Applied Approach* (Springer, Berlin, 2021)
- [13] M. Giustina, A. Mech, S. Ramelow, et al., Bell violation using entangled photons without the fair-sampling assumption, *Nature* **497**, 227 (2013)
- [14] B. G. Christensen, K. T. McCusker, J. Altepeter, et al., Detection-Loophole-Free Test of Quantum Nonlocality, and Applications, *Phys. Rev. Lett.* **111**, 130406 (2013)
- [15] T. Scheidl, R. Ursin, J. Kofler, et al., Violation of local realism with freedom of choice, *Proc. Nat. Acad. Sci.* **107**, 19708 (2010)
- [16] Zh. Li *et al.*, Testing Real Quantum Theory in an Optical Quantum Network, *Phys. Rev. Lett.* **128**, 040402 (2022)
- [17] M. Chen *et al.*, Ruling Out Real-Valued Standard Formalism of Quantum Theory, *Phys. Rev. Lett.* **128**, 040403 (2022)
- [18] J. L. Lancaster, N. M. Palladino, Testing the necessity of complex numbers in quantum mechanics with IBM quantum computers, arXiv:2205.01262
- [19] D. Wu *et al.*, Experimental Refutation of Real-Valued Quantum Mechanics under Strict Locality Conditions, *Phys. Rev. Lett.* **129**, 140401 (2022)
- [20] A. Bednorz, J. Batle, Optimal discrimination between real and complex quantum theories, *Phys. Rev. A* **106**, 042207 (2022).
- [21] J. Yao, H. Chen, Y.-L. Mao, Zh.-D. Li, J. Fan, Proposals for ruling out the real quantum theories in an entanglement-swapping quantum network with causally independent sources, arXiv:2312.14547
- [22] European Organization For Nuclear Research and Open AIRE, Zenodo, CERN, 2021, <https://doi.org/10.5281/zenodo.11112360>
- [23] L. Vandenberghe and S. Boyd, Semidefinite programming, *SIAM Review* **38**, 49 (1996).
- [24] J. Koch, T. M. Yu, J. Gambetta, A. A. Houck, D. I. Schuster, J. Majer, Alexandre Blais, M. H. Devoret, S. M. Girvin, R. J. Schoelkopf, *Phys. Rev. A* **76**, 042319 (2007)
- [25] David C. McKay, Christopher J. Wood, Sarah Sheldon, Jerry M. Chow, Jay M. Gambetta *Phys. Rev. A* **96**, 022330 (2017)